Chemical Equilibrium Modeling for Magnetite-Packed Crevice Chemistry in a Nuclear Steam Generator

Chi Bum Bahn,* In Hyoung Rhee,† Il Soon Hwang, and Byunggi Park

*Department of Nuclear Engineering, Seoul National University, Seoul 151-742, Korea. *E-mail: bcb@snu.ac.kr*
†Department of Chemical Engineering, Soonchunhyang University, Asan, Chungnam 336-745, Korea
Received March 11, 2005

Modeling of a steam generator crevice in a nuclear power system needs to take into account both thermal-hydraulic and chemical phenomena. As a first step towards developing a reliable model, a chemical equilibrium model was developed to predict chemical speciation in a magnetite-packed crevice by adopting the "tableau" method. The model was benchmarked with the available experimental data and the maximum deviation did not exceed two orders of magnitude. The developed model was applied to predict the chemical speciation in a magnetite-packed crevice. It was predicted that caustic environment was developed by the concentration of NaOH and the dissolution of magnetite. The model indicated that the dominant aqueous species of iron in the caustic crevice was FeO_2^-. The increase of electrochemical corrosion potential observed in the experiment was rationalized by the decrease of dissolved hydrogen concentration due to a boiling process. It was predicted that under the deaerated condition magnetite was oxidized to hematite.

Key Words : Chemical equilibrium model, Tableau method, Steam generator crevice, Magnetite, NaOH concentration

Introduction

In a locally restricted geometry on the secondary side of steam generator (SG) in a pressurized water reactor (PWR), impurities in bulk water can be concentrated by boiling processes to extreme pH that may then accelerate the corrosion of tubing and adjacent materials.

A detailed model of the transport processes that produce concentrated solutions locally in PWR SG's has been developed by Millett and Fenton.[1,2] The model describes the heat, mass, and momentum transfer processes that occur in porous deposits such as those found in tube support plate (TSP), tubesheet crevices and the sludge pile on top of the tubesheet. The model is used to predict the concentration of a species in the pore solution. The model predictions are compared to available experimental data. The model is in excellent agreement with the carbon fiber packed crevice data. Millett's model is based on thermal-hydraulic relations, but it does not consider the chemical and electrochemical properties. Therefore the electrochemical potential or pH in crevices cannot be predicted.

A new model for describing transport processes in PWR SG tube/TSP crevices has been developed by Engelhardt *et al.*[3,4] Based on Millett's model, Engelhardt's model includes the influence of convective transport, diffusion, and migration of species in the crevice on the evolution of crevice properties. Another localized electrochemical model has been developed by Fauchon.[5] The model considers a two-phase countercurrent flow of water and steam within a porous deposit, driven by capillary forces. Convection and diffusion processes are taken into account. Several homogeneous reactions are considered as well as electrochemical reactions. The model predictions showed that the crevice is initially steam-blanketed and slowly becomes wetted as the concentrated liquid with higher boiling point migrates into the steam-blanketed region. Engelhardt's and Fauchon's models consider a few chemical reactions and species but it includes only Fe^{2+}, $FeOH^+$, Na^+, Cl^-, H^+, and OH^-. At the wide ranges of pH, various dissolved species of iron can be present in a crevice, such as $HFeO_2^-$, FeO(aq), FeO_2^-, or Fe(OH)O(aq). To evaluate the crevice chemistry realistically, chemical model such like MULTEQ® [6,7] can be combined with the current available thermal-hydraulic models, which makes it possible to take into account the thermal-hydraulic and chemical phenomena. But as a first step towards developing the combined model, a chemical equilibrium model that predicts the chemical speciation in a magnetite-packed crevice under an equilibrium state was developed. Another objective is to compile available thermodynamic database applicable at higher temperature especially for iron species and verify MULTEQ® database which is widely used in a nuclear industry. By using the equilibrium model, it was tried to analyze the experimental data.

Numerical Model

A. Model Description. In order to develop a model which can calculate the chemical speciation in a magnetite-packed crevice, the "tableau" method was adopted.[8] The "tableau" methodology is a convenient way to express the stoichiometric relations between species and components. In order to write a complete set of equations – mole balances and the mass action laws – for the equilibrium composition of this system, it is convenient to organize all information into a "tableau". To simulate the magnetite-packed crevice condition, four ferrous ions and six ferric ions were considered.

Table 1. The relationship between species and components obtained by using the "tableau" method

#	Species	H^+	H_2(aq)	Na^+	Fe^{2+}	$\log_{10} K$
1	H^+	1	0	0	0	0
2	OH^-	−1	0	0	0	$\log_{10} K_w$
3	H_2(g)	0	1	0	0	$\log_{10} K_{H_2}$
4	H_2(aq)	0	1	0	0	0
5	Na^+	0	0	1	0	0
6	NaOH(aq)	−1	0	1	0	$\log_{10} K_6 + \log_{10} K_w$
7	Fe^{2+}	0	0	0	1	0
8	$FeOH^+$	−1	0	0	1	$\log_{10} K_8$
9	FeO(aq)	−2	0	0	1	$\log_{10} K_9$
10	$HFeO_2^-$	−3	0	0	1	$\log_{10} K_{10}$
11	Fe^{3+}	1	−1/2	0	1	$-\frac{1}{2}\log_{10} K_{11} - \frac{1}{2}\log_{10} K_{H_2}$
12	$FeOH^{2+}$	0	−1/2	0	1	$\log_{10} K_{12} - \frac{1}{2}\log_{10} K_{11} - \frac{1}{2}\log_{10} K_{H_2}$
13	FeO^+	−1	−1/2	0	1	$\log_{10} K_{13} - \frac{1}{2}\log_{10} K_{11} - \frac{1}{2}\log_{10} K_{H_2}$
14	$Fe_2(OH)_2^{4+}$	0	−1	0	2	$\log_{10} K_{14} - \log_{10} K_{11} - \log_{10} K_{H_2}$
15	Fe(OH)O(aq)	−2	−1/2	0	1	$\log_{10} K_{15} - \frac{1}{2}\log_{10} K_{11} - \frac{1}{2}\log_{10} K_{H_2}$
16	FeO_2^-	−3	−1/2	0	1	$\log_{10} K_{16} - \frac{1}{2}\log_{10} K_{11} - \frac{1}{2}\log_{10} K_{H_2}$
17	Fe_3O_4(s)	−6	−1	0	3	$-\log_{10} K_{17} - \log_{10} K_{H_2}$
18	Fe_2O_3(s)	−4	−1	0	2	$-\log_{10} K_{18} - \log_{10} K_{H_2}$
	H_2(aq)	0	1	0	0	0.0001 mol/kg
	NaOH	−1	0	1	0	0.00217 mol/kg
	Fe_3O_4	−6	−1	0	3	10.0 mol/kg

For the evaluation of the results from caustic crevice experiments, Na^+ and NaOH(aq) were also included. From eighteen species, taking H^+, H_2(aq), Na^+, and Fe^{2+} implicitly as components yields Table 1. Table 1 contains all the necessary information for the equilibrium problem and a complete set of equations is readily written for mole balances from each component's column. Firstly, the mass action laws (from each row) are obtained to produce Table 1. There are eighteen unknowns in this equilibrium problem (the concentrations of the species) and eighteen equations (four mole balances and fourteen mass laws).

The "tableau" method assumes that the system of interest is in a chemical equilibrium state and a closed system. However, the chemical conditions in crevices depend on several factors like convection, diffusion, migration and chemical reactions. Also, heat and mass transfer occur across the system boundary. However, if the crevice conditions are in a stationary state and NaOH concentration is high enough as compared with the iron species' concentration, it is thought that a chemical equilibrium method like the "tableau" method can be applied to the prediction of the crevice chemical conditions.

B. Numerical Methods. In the case of the present problem, four nonlinear equations composed of the components, H^+, H_2(aq), Na^+, and Fe^{2+}, can be formulated. To solve the system of nonlinear equations, the Newton's method was adopted.[9] Figure 1 shows the flow chart of the chemical equilibrium model used to calculate the chemical speciation in a magnetite-packed crevice. Iteration for computing the Jacobian matrix was repeated until the convergence criteria was achieved or the number of iteration exceeded a predefined maximum value. The convergence of boiling point elevation was also confirmed by introducing another iteration loop. The boiling point elevation at each step was calculated from the concentrations of species and compared with that of previous step until the difference became small enough.

Results and Discussions

A. Thermodynamic Database. To calculate the concentration of species by using "tableau" method, the equilibrium constant should be known as a function of temperature. As a thermodynamic database, MULTEQ® database[6] and HSC Chemistry®[10] can provide the high temperature thermodynamic data for iron species. MULTEQ® is widely used in a nuclear industry, which contains a lot of data for various kinds of species and calculates ionic concentrations under the chemical equilibrium conditions. HSC Chemistry® can calculate the partial molal Gibbs energy of ionic species as a function of temperature by using the revised HKF model.[11-14] The equilibrium constants calculated from two thermo-

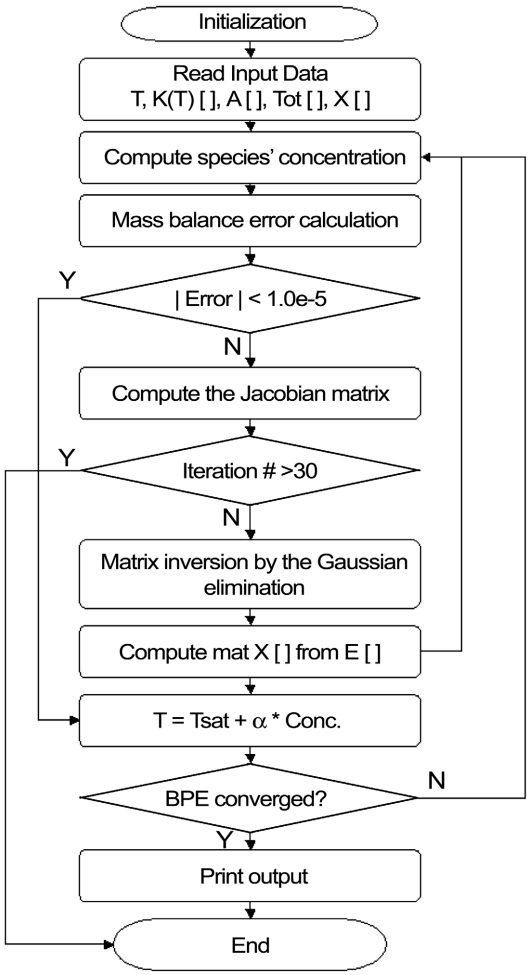

Figure 1. Flow chart of the chemical equilibrium model used to calculate the chemical speciation in a magnetite-packed crevice.

dynamic databases were compared with available experimental data. Through these comparisons, the accuracy of each database was evaluated.

For the equilibrium constants of reactions related to Fe^{2+} and $FeOH^{+}$, the thermodynamic databases and experimentally derived data by Sweeton and Baes[15] showed similar trend from 0 to 300 °C. The maximum difference did not exceed four orders of magnitude. Figure 2 shows the equilibrium constant for Eq. (1) as a function of temperature.

$$Fe_3O_4 + H_2(g) = 3FeO(aq) + H_2O \quad (1)$$

In Figure 2, the equilibrium constants from HSC Chemistry® and experimental data slightly increased with temperature but MULTEQ® database showed different behavior with temperature. At 300 °C, the maximum difference between each data was about six orders of magnitude. Figure 3 shows the equilibrium constant for Eq. (2) as a function of temperature.

$$Fe_3O_4 + H_2(g) + 2H_2O = 3HFeO_2^- + 3H^+ \quad (2)$$

All of three data slightly increased with temperature but at 300 °C the maximum difference between each data exceeded thirty orders of magnitude. As described in Figure 3,

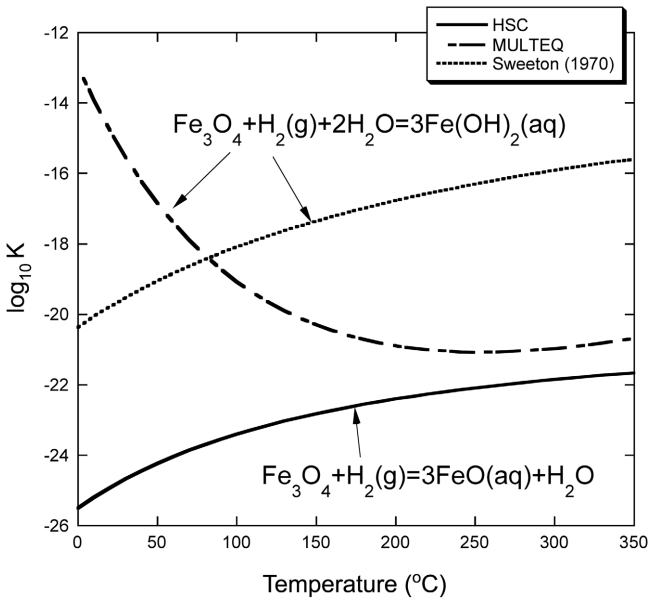

Figure 2. Comparison of the equilibrium constants as a function of temperature for FeO(aq).

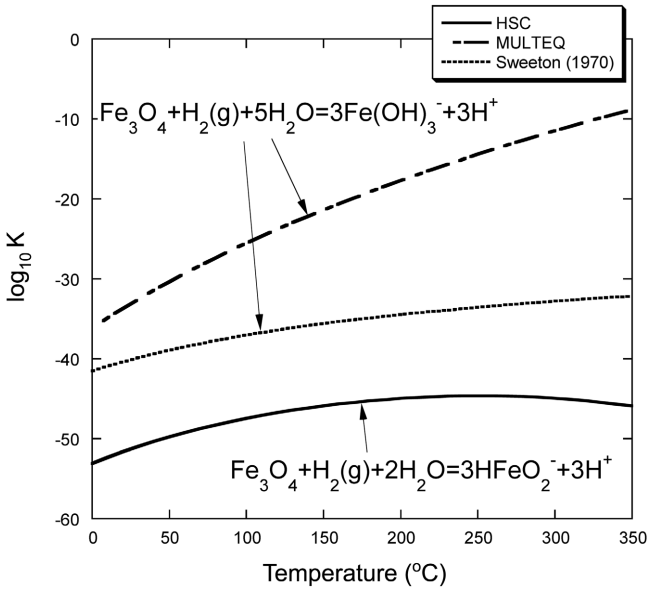

Figure 3. Comparison of the equilibrium constants as a function of temperature for $HFeO_2^-$.

MULTEQ® database can overestimate the concentration of $HFeO_2^-$ ion, especially at higher temperature.

In case of ferric ions, the equilibrium constants related to the reactions of Fe^{3+}, $FeOH^{2+}$, and FeO^{+} showed similar trend with temperature from 0 to 300 °C. The maximum difference between two databases and the experimental data was less than two orders of magnitude. For Fe(OH)O(aq), there was no available database or experimental data except HSC Chemistry®. Figure 4 shows the equilibrium constant for Eq. (3) as a function of temperature.

$$Fe_2O_3 + H_2O = 2FeO_2^- + 2H^+ \quad (3)$$

In Figure 4, HSC Chemistry® database were compared with

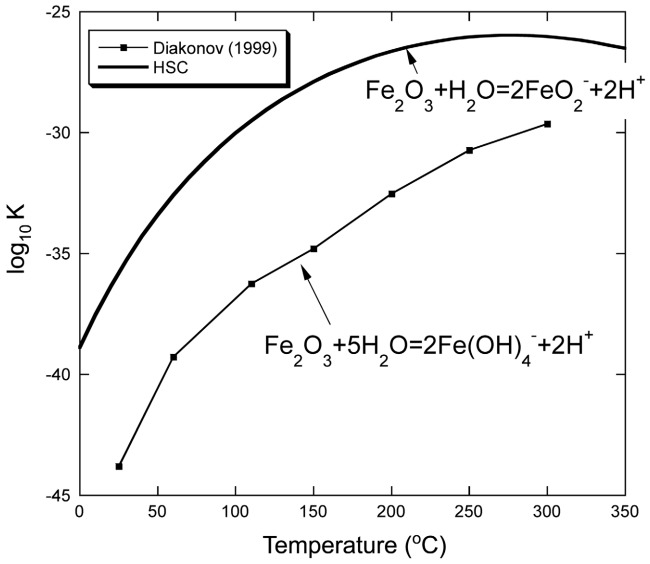

Figure 4. Comparison of the equilibrium constants as a function of temperature for FeO_2^- between HSC Chemistry® database and experimentally derived data.

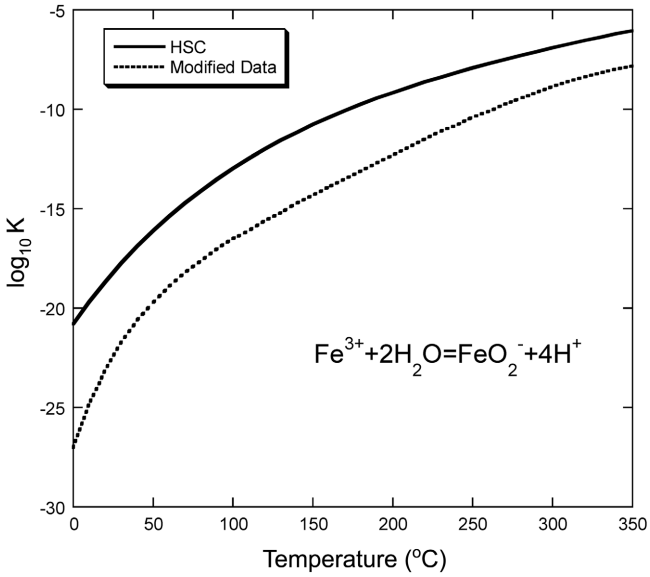

Figure 5. Comparison of the equilibrium constants as a function of temperature between original HSC Chemistry® database and modified database.

the data derived from experimental results by Diakonov *et al.*[16] The temperature dependency showed a similar behavior but the difference between the database and the experimental results at 300 °C was about four orders of magnitude. As described in Figure 6 and 7, HSC Chemistry® exaggerated the concentration of FeO_2^- ion. This problem was discussed in a later section. Figure 5 shows two equilibrium constant variation curves: one is the curve for Eq. (4) calculated from original HSC Chemistry® database and the other is calculated from modified HSC Chemistry® database.

$$Fe^{3+} + 2H_2O = FeO_2^- + 4H^+ \quad (4)$$

The database modification only for FeO_2^- ion was conducted

Table 2. Summary of coefficients for each reaction's equilibrium constant

	A[1)]	B	C	D	E
K_w	42705	−799.85	−0.12421	287.85	−2.8988e+6
K_{H_2}	−2573.6	56.071	2.2895e-4	−17.986	6908.3
K_6	−51402	925.83	0.14043	−335.36	3.0478e+6
K_8	−20620	320.27	0.047047	−115.75	1.0633e+6
K_9	−39380	618.99	0.092605	−224.67	1.8678e+6
K_{10}	745.05	−165.42	−0.031102	59.791	−4.4318e+5
K_{11}	−48681	984.11	0.15073	−353.45	3.0973e+6
K_{12}	−28361	488.22	0.071623	−175.04	1.4673e+6
K_{13}	−44322	780.95	0.11418	−280.99	2.0717e+6
K_{14}	−1.2504e+5	2235.7	0.33562	−809.27	7.0115e+6
K_{15}	−61641	1094.1	0.15658	−393.45	2.7506e+6
K_{16}	−30921	468.53	0.061054	−166.57	9.7195e+5
K_{17}	1.1522e+5	−1843.7	−0.27457	662.56	−5.6772e+6
K_{18}	78089	−1237.5	−0.18336	444.4	−3.7977e+6

[1)] $\log_{10} K = \frac{A}{T} + B + CT + D \log 10\ T + \frac{E}{T^2}$, $T(K)$

by adopting the experimentally derived data by Diakonov as described in Figure 4. From the results of thermodynamic database survey, only HSC Chemistry® can provide data for all ferric and ferrous ions. Table 2 represents the summary of coefficients for each reaction's equilibrium constant that are obtained from HSC Chemistry® Version 4.0. The original data of equilibrium constant was fitted by using the appropriate equation described in Table 2.

The calculation results based on HSC Chemistry® were benchmarked with experimentally observed data. The iron solubility at 300 °C was calculated as a function of KOH concentration as shown in Figure 6. Experimental data by Sweeton and Baes[15] was located between HSC Chemistry®

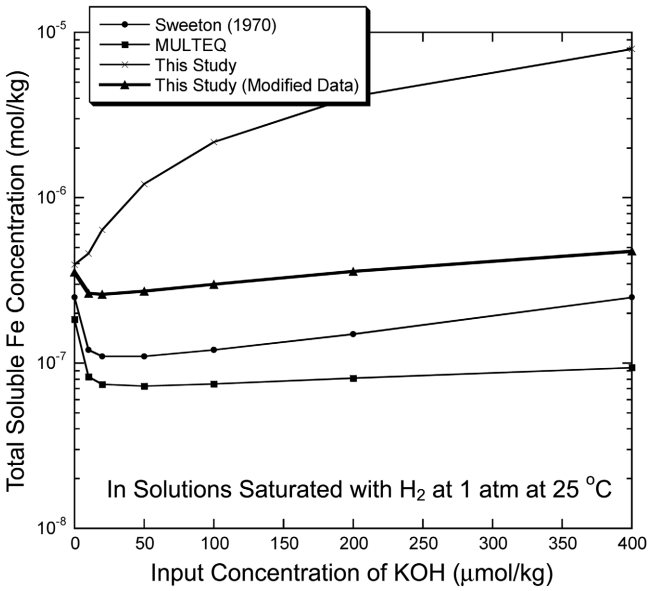

Figure 6. Predicted iron solubility as a function of KOH concentration at 300 °C compared with experimentally observed data.

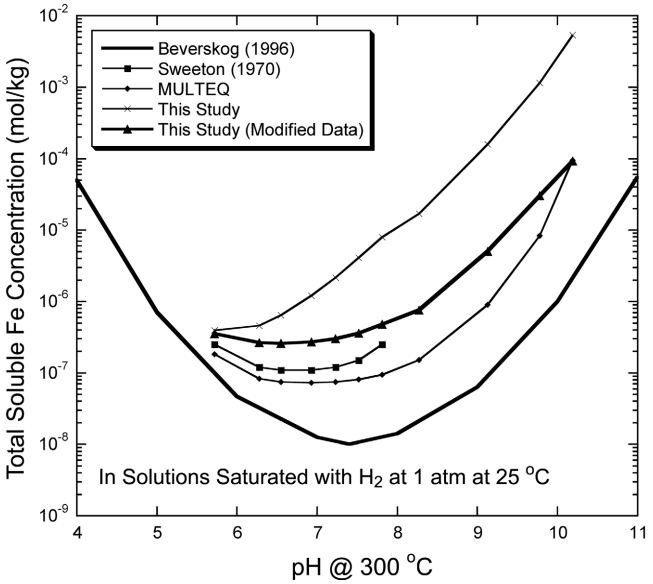

Figure 7. Predicted iron solubility as a function of pH at 300 °C compared with experimentally observed data.

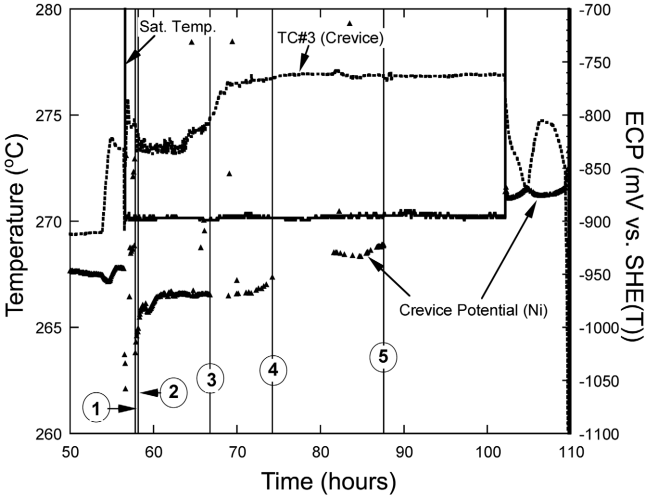

Figure 8. Crevice temperature and Ni electrode potential at specific times of interest to analyze the crevice chemistry.

and MULTEQ® database. In Figure 6, 'Modified Data' means the calculation results obtained with the modified equilibrium constant data for FeO_2^- ion. After the database modification, the results showed very similar behavior to the experimental data and MULTEQ® database. From these results, it is found that the original HSC Chemistry® database overestimates the concentration of FeO_2^- ion. Figure 7 shows the total soluble iron concentration as a function of pH at 300 °C. The data by Beverskog and Puigdomenech[17] was the lower boundary and HSC Chemistry® database was upper boundary. From Figure 7, it is confirmed that the original HSC Chemistry® database overestimates the iron solubility under alkaline and caustic environments. However, the calculation results with the modified database showed a good agreement with other experimental and calculated data. Since this study is interested in the solubility and speciation of iron species under caustic solution, the calculation results under acid environments were not considered. As shown in Figure 7, the maximum difference for iron solubility at 300 °C was less than two orders of magnitude.

B. Chemical Speciation in Crevice. The developed equilibrium model was applied to predict the chemical speciation for experimentally simulated crevice environments. A simulated crevice was instrumented with thermocouples and electrodes to measure temperature and electrochemical potential variations, respectively. The crevice was initially packed with magnetite powder to produce a realistic crevice environment. The temperature difference between the primary water and the secondary saturation temperature was 20 °C, which induces the heat transfer from primary to secondary water and the boiling on the surface of primary tubing and in the crevice. Detail conditions and analysis of experimental results were described in earlier work by authors.[18,19] The measured temperature and Ni electrode potential in the crevice at specific times of interest were shown in Figure 8. At each specific time, $[NaOH]_T$ in a recipe, as shown in Table 1, was determined from the measured temperature. It was assumed that the boiling point elevation is linearly proportional to the concentration of NaOH, which can be calculated from the temperature elevation and a proportional constant. The concentrations of magnetite and dissolved hydrogen in the recipe maintained constant values, as shown in Table 1. However, to make the calculated hydrogen electrode potential correspond to the measured potential, the Henry's law constant of hydrogen was modified by multiplying arbitrary constant. The modification of the Henry's law constant can be interpreted as a method considering the hydrogen stripping from the crevice due to the boiling process. The dissolved hydrogen concentration will be continuously decreased if the considering system is an open system, not closed one, which leads to the escape of gaseous phase like hydrogen or steam from the crevice. As described in the 'Model Description' section, it was assumed that the crevice environments were in a stationary state. Even if there were concentration variations with time, the reaction kinetics are so fast as compared with the variations that the equilibrium state assumption could be applied. It was assumed that the Ni electrode behaves as a hydrogen electrode and the measured potential is dependent on the solution pH and the dissolved hydrogen. The possibility of the mixed potential was excluded for the sake of simple calculation.

Figure 9(a) shows the variation of pH and the dissolved hydrogen concentration and Figure 9(b) shows the corresponding potential at each time of interest. $[H_2(aq)]$ in the recipe was 10^{-4} mol/kg, but the calculated $[H_2(aq)]$ was decreased down to $10^{-7.5}$ mol/kg. Considering that the distribution coefficient of hydrogen at 270 °C was about 200, the calculated ratio of initial hydrogen content to the content under boiling condition was higher than the distribution coefficient. If the measured potential represents the hydrogen electrode potential, it means that there is an

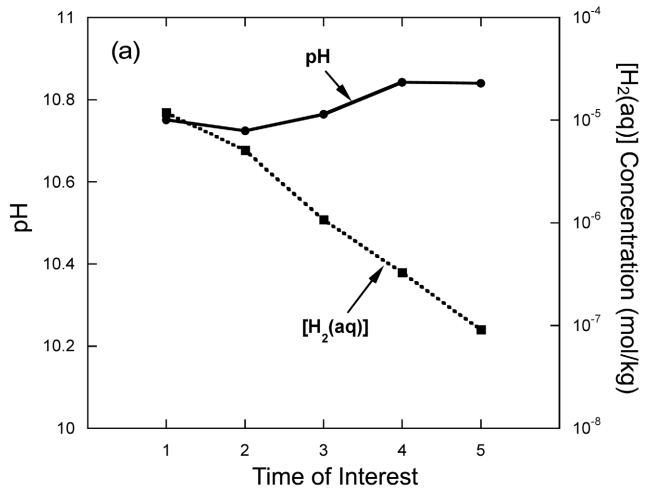

	1	2	3	4	5
[NaOH] mol/kg	1.83	1.64	1.94	2.70	2.67
[Fe3O4] mol/kg	10	10	10	10	10.

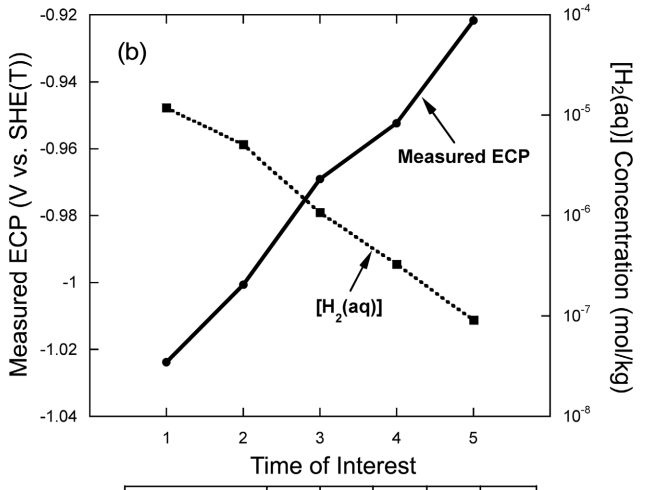

	1	2	3	4	5
[NaOH] mol/kg	1.83	1.64	1.94	2.70	2.67
[Fe3O4] mol/kg	10	10	10	10	10.

Figure 9. (a) Variation of pH and dissolved hydrogen concentration and (b) variation of measured ECP and dissolved hydrogen concentration.

additional path of hydrogen escape from the liquid phase as compared with the expected value from the distribution coefficient. A real crevice situation is not a closed system and hydrogen can escape from the crevice with the vapor phase. More reasonable method to consider the effects of volatile species, such as hydrogen, hydrazine, or hydrochloric acid is necessary.

Figure 10 shows the concentration of iron oxide and dissolved sodium species in the magnetite-packed crevice at the specific times described in Figure 8. As shown in Figure 10, the some magnitude of magnetite was transformed to hematite. It was interpreted that the decrease of the dissolved hydrogen concentration caused the relatively oxidizing environment and it led to the transformation of magnetite. Unfortunately, the magnetite powder was not analyzed after

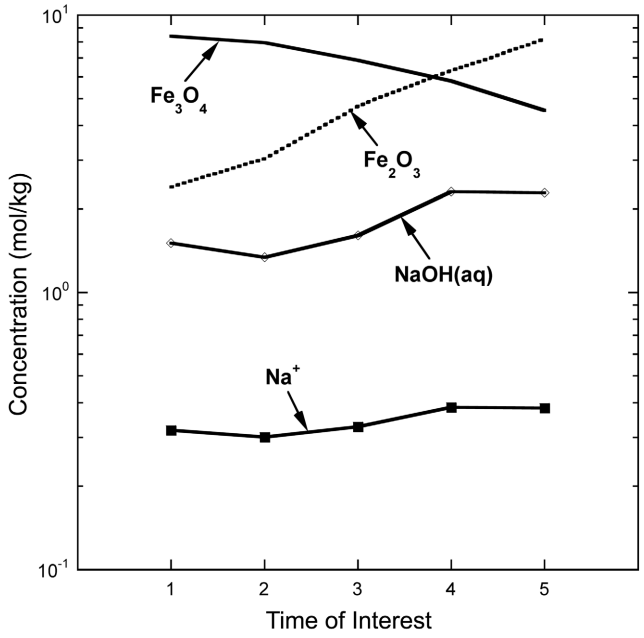

	1	2	3	4	5
[NaOH] mol/kg	1.83	1.64	1.94	2.70	2.67
[Fe3O4] mol/kg	10	10	10	10	10.

Figure 10. Variation of the concentration in the magnetite-packed crevice for iron oxide and dissolved sodium species.

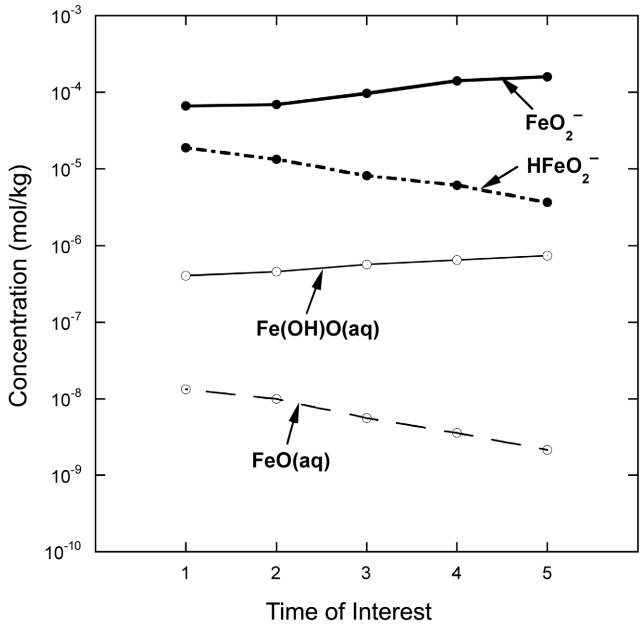

	1	2	3	4	5
[NaOH] mol/kg	1.83	1.64	1.94	2.70	2.67
[Fe3O4] mol/kg	10	10	10	10	10.

Figure 11. Variation of dissolved species' concentration in the magnetite-packed crevice.

the experiment. Therefore, more experimental study is needed to confirm the possibility of magnetite transformation into hematite under deaerated crevice environments. NaOH(aq) was thermodynamically more stable element than

Na^+ under the strong alkaline environment. Figure 11 shows the variation of dissolved iron species' concentration in the magnetite-packed crevice. As shown in Figure 11, the most abundant dissolved iron species is FeO_2^-, as was expected. The concentrations of iron anions were much higher than those of iron cations because of the caustic crevice environment caused by NaOH concentration. As the hydrogen concentration decreased, the concentration of dissolved Fe(III) species, such as FeO_2^- and Fe(OH)O(aq), increased while those of dissolved Fe(II) species, such as $HFeO_2^-$ and FeO(aq) decreased.

Summary and Conclusion

From this study, following conclusions are made:

1. To compute the chemical equilibrium in a magnetite-packed crevice environment, a chemical equilibrium model was developed by adopting the "tableau" method.

2. The available thermodynamic databases for iron species were compiled and the accuracy of each database was evaluated. Through these processes, it was found that MULTEQ® can overestimate $HFeO_2^-$ ion concentration under the caustic environments, which can be occurred in a magnetite-packed crevice.

3. HSC Chemistry® database for soluble iron species was selected as main thermodynamic database, which was modified with experimentally observed results for FeO_2^- ion. The predicted iron solubility with the modified HSC Chemistry® database was benchmarked with available experimental data from neutral to caustic environments at 300 °C. The predicted results showed a similar behavior to other data and the maximum deviation was less than two orders of magnitude.

4. The developed model was applied to predict the chemical speciation in a magnetite-packed crevice. Experimentally, caustic crevice chemistry was developed by concentration of NaOH and it led to the dissolution of magnetite. The dominant aqueous species of iron in the caustic crevice was FeO_2^-. The increase in ECP during the packed crevice test was rationalized by the decrease of dissolved hydrogen concentration by boiling process.

5. At the condition of low dissolved hydrogen, it was predicted that magnetite was transformed to hematite in an equilibrium state.

Acknowledgements. This work has been financially supported by the National Research Laboratory program of the Korean Ministry of Science and Technology, and the Nuclear Transmutation Energy Research Center program of the Korean Ministry of Commerce, Industry and Energy.

References

1. Millett, P. J. *Theoretical and Experimental Investigation of Local Concentration Processes in PWR Steam Generators,* Ph. D. Dissertation; The University of Connecticut: CT, U.S.A., 1991.
2. Millett, P. J.; Fenton, J. M. *Nucl. Tech.* **1994**, *108*, 256.
3. Engelhardt, G. R.; Macdonald, D. D. *Corr. Sci.* **1999**, *41*, 2165.
4. Engelhardt, G. R.; Macdonald, D. D.; Millett, P. J. *Corr. Sci.* **1999**, *41*, 2191.
5. Fauchon, C. L. *Development and Testing of an Electrochemical Model for PWR Steam Generators Crevice Environment*, Master Thesis; Massachusetts Institute of Technology: Cambridge, U.S.A., 2000.
6. Paine, J. P. N. *MULTEQ: Equilibrium of an Electrolytic Solution with Vapor-Liquid Partitioning and Precipitation, Volume 2: The Database (Revision 3)*, NP-5561-CCML, Volume 2, Revision 3; Electric Power Research Institute: San Hose, U.S.A., 1992.
7. Paine, J. P. N.; Millett, P. J. *MULTEQ: Equilibrium of an Electrolytic Solution with Vapor-Liquid Partitioning, Volume 3: Theory Manual,* NP-5561-CCML Volume 3; Electric Power Research Institute: San Hose, U.S.A., 1992.
8. Morel, F. M. M.; Hering, J. G. *Principles and Applications of Aquatic Chemistry*; John Wiley & Sons: New York, U.S.A., 1983; p 11.
9. Kim, C. H. *Numerical Methods and Computer Programming (in Korean)*; Kyohaksa: Seoul, Korea, 1990; p 262.
10. Roine, A. *HSC Chemistry® for Windows: Chemical Reaction and Equilibrium Software with Extensive Thermochemical Database, User's Guide*, Version 5.0; Outokumpu: PORI, Finland, 2002.
11. Shock, E. L.; Helgeson, H. C. *Geochim. Cosmochim. Acta* **1988**, *52*, 2009.
12. Shock, E. L.; Helgeson, H. C.; Sverjensky, D. A. *Geochim. Cosmochim. Acta* **1989**, *53*, 2157.
13. Shock, E. L.; Oelkers, E. H.; Johnson, J. W.; Sverjensky, D. A.; Helgeson, H. C. *J. Chem. Soc. Faraday Trans.* **1992**, *88*, 803.
14. Shock, E. L.; Sassani, D. C.; Willis, M.; Sverjensky, D. A. *Geochim. Cosmochim. Acta* **1997**, *61*, 907.
15. Sweeton, F.; Baes, C. *J. Chem. Thermodynamics* **1970**, *2*, 479.
16. Diakonov, I. I.; Schott, J.; Martin, F.; Harrichourry, J.-C.; Escalier, J. *Geochim. Cosmochim. Acta* **1999**, *63*, 2247.
17. Beverskog, B.; PUIGDOMENECH, I. *Corr. Sci.* **1996**, *38*, 2121.
18. Bahn, C. B.; Oh, S. H.; Park, B. G.; Hwang, I. S.; Rhee, I. H.; Kim, U. C.; Na, J. W. *Nucl. Eng. Des.* **2003**, *225*, 129.
19. Bahn, C. B.; Oh, S. H.; Park, B. G.; Hwang, I. S.; Rhee, I. H.; Kim, U. C.; Na, J. W. *Nucl. Eng. Des.* **2003**, *225*, 145.